AD A034070

REPORT NVL-0059-002

MONTE CARLO STUDIES OF HOT-ELECTRON DISTRIBUTIONS IN THIN INSULATING FILMS: II. ENERGY DEPENDENT MEAN FREE PATH AND INSTABILITY

S. Baidyaroy, M. A. Lampert, B. Zee, and Ramon U. Martinelli

PRINCETON UNIVERSITY
Department of Electrical Engineering
Princeton, New Jersey 08540
Principal Investigator: Walter C. Johnson
Telephone: (609) 452-4621

15 November 1976

SPECIAL TECHNICAL REPORT NO. 1

Approved for public release; distribution unlimited.

Prepared for:

NIGHT VISION LABORATORY
U. S. Army Electronics Command
Fort Belvoir, Virginia 22060

Sponsored by:

DEFENSE ADVANCED RESEARCH PROJECTS AGENCY

DARPA Order No. 2182
Program Code No. 6D10
Contract DAAG53-76-C-0059
Effective Date: 17 November 1975
Expiration Date: 31 December 1977

DDC
RECEIVED
JAN 6 1977
A

The views and conclusions contained in this document are those of the authors and should not be interpreted as necessarily representing the official policies, either expressed or implied, of the Defense Advanced Research Projects Agency of the U. S. Government.

Unclassified

SECURITY CLASSIFICATION OF THIS PAGE (When Data Entered)

REPORT DOCUMENTATION PAGE	READ INSTRUCTIONS BEFORE COMPLETING FORM
1. REPORT NUMBER: NVL-0059-002	2. GOVT ACCESSION NO.: Special Technical Rept. No. 1
3. RECIPIENT'S CATALOG NUMBER	
4. TITLE (and Subtitle): MONTE CARLO STUDIES OF HOT-ELECTRON DISTRIBUTIONS IN THIN INSULATING FILMS: II. ENERGY DEPENDENT MEAN FREE PATH AND INSTABILITY.	5. TYPE OF REPORT & PERIOD COVERED: # #
	6. PERFORMING ORG. REPORT NUMBER
7. AUTHOR(s): S. Baidyaroy, M. A. Lampert, B. Zee, Ramon U. Martinelli	8. CONTRACT OR GRANT NUMBER(s): DAAG53-76-C-0059; ARPA Order-2182
9. PERFORMING ORGANIZATION NAME AND ADDRESS: Princeton University, Princeton, NJ 08540; Principal Investigator: Walter C. Johnson; Telephone: (609) 452-4621	10. PROGRAM ELEMENT, PROJECT, TASK AREA & WORK UNIT NUMBERS: 61101E, ARPA 2182, 6D10, 024CJ
11. CONTROLLING OFFICE NAME AND ADDRESS: Defense Advanced Research Projects Agency, 1400 Wilson Boulevard, Arlington, Virginia 22209	12. REPORT DATE: 15 Nov 1976; NUMBER OF PAGES: 23
14. MONITORING AGENCY NAME & ADDRESS (if different from Controlling Office): Night Vision Laboratory, DRSEL-NV-II, Fort Belvoir, Virginia 22060	15. SECURITY CLASS. (of this report): Unclassified
	15a. DECLASSIFICATION/DOWNGRADING SCHEDULE

16. DISTRIBUTION STATEMENT (of this Report)

Approved for public release; distribution unlimited.

17. DISTRIBUTION STATEMENT (of the abstract entered in Block 20, if different from Report)

18. SUPPLEMENTARY NOTES

The work reported herein is a continuation of research initiated under ARPA Order No. 2180, monitored by Air Force Cambridge Research Laboratories (LQ). This report is a preprint of a paper submitted to the Journal of Applied Physics.

19. KEY WORDS (Continue on reverse side if necessary and identify by block number)

Hot electrons
Hot-electron transport
High-field transport
Insulating films

20. ABSTRACT (Continue on reverse side if necessary and identify by block number)

A Monte Carlo study has been made of hot electron energy distributions in thin insulating films. Whereas a constant energy-independent mean free path results in a stable energy distribution, it is shown that an energy-dependent mean free path which increases with increasing energy can lead to energetic runaway of the electrons. A graphical method has been developed to gain insight into this problem, and is illustrated by several prototypical examples.

DD FORM 1 JAN 73 1473 EDITION OF 1 NOV 65 IS OBSOLETE
S/N 0102-014-6601

Unclassified
SECURITY CLASSIFICATION OF THIS PAGE (When Data Entered)

400 734

Monte Carlo Studies of Hot-Electron Energy Distributions in Thin Insulating Films: II. Energy-Dependent Mean Free Path and Instability*

By

S. Baidyaroy,† M. A. Lampert,†† and B. Zee¶
Department of Electrical Engineering
Princeton University
Princeton, New Jersey 08540

And

Ramon U. Martinelli
RCA Laboratories
Princeton, New Jersey 08540

ABSTRACT

Monte Carlo calculations are used to study theoretically hot electron transport through a thin insulating film subjected to a high, uniform electric field F. A constant energy-independent mean free path λ leads to a stable, steady-state energy distribution for the electrons, characterized by an average steady-state energy $E_{av,ss}$. $E_{av,ss}$ depends on λ, F and ε_{ph}, the optical phonon energy associated with scattering of the hot electrons by the lattice. An energy-dependent mean free path $\lambda(E)$ which increases with increasing electron energy can lead to energetic runaway of either a relatively small number of electrons in the distribution (quasi-stability, or a bi-modal distribution) or the entire distribution (instability). A graphical method has been developed to gain insight into this problem. The method rests on an analysis of the interactions of two curves plotted in the E, λ plane, one curve being the plot of $E_{av,ss}$ vs. λ where λ is the mean-free-path parameter taken to be constant (energy-independent) for each calculation of $E_{av,ss}$, the other curve being the plot of the actual functional dependence of λ on E, $\lambda(E)$. The method is illustrated by several prototypical examples.

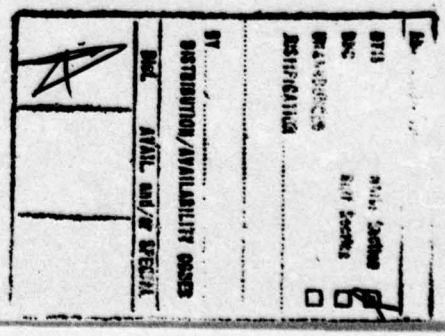

I. Introduction

In a previous paper,[1] the authors studied theoretically, using Monte Carlo techniques, hot-electron transport through thin insulating films in the presence of high, applied electric fields, on the order of a megavolt per centimeter. This study has particular relevance to contemporary solid-state electronics, where thin insulating layers, usually on a silicon substrate, are frequently subjected to electric fields near the threshold for electrical breakdown. The previous paper, hereafter referred to as I, studied transport characterized by a constant, energy-independent mean free path (mfp) between collisions with the lattice. The major result found is that the constant-mfp constraint always leads to a stable, steady-state energy distribution no matter how anisotropic the microscopic scattering process may be, short of pure forward scattering. Further, the average energy of the steady-state distribution is given by a simple scaling law, namely, Eq. (1) of the present paper.

In the present paper we study hot-electron transport characterized by an energy-dependent mfp, namely, one which increases with increasing electron energy. This latter property is relevant to the electrical breakdown problem, since it favors runaway, in energy, of either a small number of electrons[2] or, in some cases, of the entire energy distribution. Both of these situations are examined in the present paper. In particular, we exhibit a powerful graphical technique, utilizing the previous results in I for an energy-independent mfp, to analyze the stability of the overall energy distribution where the mfp is energy-dependent, and further to obtain the average steady-state energy of the distribution when the distribution is stable.

II. Outline of the Method and the Results of I

High field, hot-electron transport is studied in an amorphous film of thickness d subjected to a uniform electric field F. The electron is injected into the film at plane z=0 in a random direction and with an initial energy E_o. Under the influence of the field it accelerates in the positive z-direction, following a Newtonian trajectory up to the point of an inelastic collision with the lattice. The length of this trajectory is determined randomly according to the functional energy dependence of the mfp. The inelastic collision process creates an optical phonon of energy ε_{ph}, and the scattered electron, therefore, emerges from the collision with an amount ε_{ph} subtracted from its energy. The new direction of motion of the electron is chosen randomly according to the functional form of the angular scattering process. We have taken the angular scattering to be dependent only on the polar angle θ with respect to the direction of travel just prior to the collision. For simplicity, we used a $(1 + \cos\theta)$-dependence to study dominant forward scattering and a $(1 - \cos\theta)$-dependence to study dominant backward scattering; isotropic scattering has no θ - dependence. With its post-collision energy and direction specified, the electron again follows a Newtonian trajectory up to its next collision with the lattice, and so on. In this manner, the electron's path through the film is followed until its emergence from the film at plane z=d, at which point the computer stores the emerging electron energy. Another electron is then injected at z=0 with energy E_o, and its path is followed in a similar manner. The process is repeated until a representative histogram of the emerging energy distribution is obtained. A minimum of 200 electrons was used to obtain the energy histograms.

In the situation studied in I, the film thickness range was on the order of one hundred to several thousand Angstroms; E_o was generally in the range 0.01 to 16 eV; F was of the order of 10^6V/cm; and ϵ_{ph} was either 0.05 or 0.1 eV--all values appropriate to the study of hot electron transport in thin films of Al_2O_3 and SiO_2.

The major result of I is as follows: For a constant mfp the distribution-in-energy for the injected electrons reaches a steady-state value, independent of the initial injection energy, for which the average steady-state energy, $E_{av,ss}$, is given by the scaling law:

$$E_{av,ss} = k(F\lambda)^2/\epsilon_{ph}, \tag{1}$$

where k is a constant determined by the details of the scattering process: the greater the probability of forward scattering, the larger the value of k. For dominant forward scattering characterized by a $(1 + \cos\theta)$ - dependence, k = 1.27; for isotropic scattering, k = 0.87; for dominant backward scattering characterized by a $(1 - \cos\theta)$ - dependence, k = 0.66. A graph of k vs. an anisotropy parameter f, defined for a simple one-dimensional random-walk simulation, is presented in Fig. 13 of I. The 'development' distance D, over which the electron energy distribution exponentially settles down to its steady-state is also given by a scaling law: $D=k'(F\lambda^2)/\epsilon_{ph}$. For a film thickness d exceeding a few D the emerging energy profile is independent of d.

We found in I that, under the constraint of constant, energy-independent mfp, any degree of forward scattering, short of exact forward scattering, leads to a finite, stable, steady-state energy distribution. Physically, this is understood as follows: For a given degree of forward scattering, particles with energies less than $E_{av,ss}$ are quickly directed along the positive z-direction by the applied field, F. This tendency to travel

with the field implies that particles with energies less than $E_{av,ss}$ are warmed up by the field. On the other hand, particles with energies greater than $E_{av,ss}$ are not significantly influenced by F and travel in nearly rectilinear trajectories. So long as there exists some chance that an energetic particle be back-scattered along the negative z-direction, such a back-scattered particle will continue traveling backwards, losing energy as it travels against the field. In the case of strong forward scattering, this backward travel is sustained, for the particle is now most likely to continue being scattered along its present course, which is the negative z-direction. This cooling effect continues until the particle is turned around by the field, or by angular scattering, into the positive z-direction Thus, an energetic balance is struck between the warming of low-energy electrons by the field and the cooling of energetic electrons by back-scattering into trajectories directed against the field. This balance produces a finite, steady-state distribution.

III. Energy-Dependent Mean Free Path; Unstable Energy Distributions and Runaway Electrons

If the mfp is energy-dependent, $\lambda = \lambda(E)$, and, further, if $\lambda(E)$ increases with increasing energy, the argument on stability presented at the end of Section II breaks down. The hotter a hot electron gets, moving, roughly, 'with' the field, the less likely it is to make any collision with the lattice. Further, even if it does make a large-angle scattering, turning it into a trajectory 'against' the field, as it subsequently undergoes cooling, the probability of its making another large-angle collision which will return it to a motion 'with' the field keeps increasing. The net effect favors higher energies for the electrons. Whether the dynamic interplay of these effects leads to full stability, as in I, or to total

instability of the distribution, with almost all electrons increasing their energy indefinitely with increasing film thickness, or to a quasi-stability with most electrons settling down within a finite steady-state distribution and a few running away in energy is the main subject of this paper.

We have studied the problem of stability, quasi-stability and instability using a graphical technique in combination with the results previously obtained in I. The quantities that are plotted graphically are E vs. λ as given by (1), where E is identified with $E_{av,ss}$ calculated as if λ were constant, and $\lambda = \lambda(E)$, the given functional dependence of λ on E. [In plotting the constant mfp scaling law (1), the quantities F and ε_{ph} must be specified, and the numerical value of k depends on the detailed form of the angular scattering law.] The properties of stability, quasi-stability and instability are analyzed in terms of the intersections of the two quantities plotted. Two simple functional forms of energy dependence of the mfp were chosen to illustrate the technique: $\lambda = \lambda_o + \alpha(E/\varepsilon_{ph})^{1/2}$ and $\lambda = \lambda_o + \beta(E/\varepsilon_{ph})$, where λ_o, α and β are adjustable constants with the dimension of length.

A. Square-root dependence of λ on E

Here we take the functional dependence of $\lambda(E)$ as

$$\lambda = \lambda_o + \alpha(E/\varepsilon_{ph})^{1/2}. \tag{2}$$

In Fig. 1, Eqs. (1) and (2) are plotted in the E-λ plane. Equation (1) is a parabola in E vs. λ, here plotted for two different values for ε_{ph}, namely 0.1 and 0.05 ev, and labelled I and II, respectively. In each case there is one, and only one, intersection between the $\lambda(E)$ parabola (2) and the scaling-law parabola (1), given analytically by the 'co-ordinates':

$$E_{av,ss} = k\frac{(F\lambda_o)^2}{\varepsilon_{ph}}\left[1 - \frac{\alpha k^{1/2} F}{\varepsilon_{ph}}\right]^{-2}, \quad \lambda = \lambda_o\left[1 - \frac{\alpha k^{1/2} F}{\varepsilon_{ph}}\right]^{-1}. \tag{3}$$

Coinciding with, or extremely close to, these points of intersection (3) in Fig. 1 are large, open circles. These circles represent direct, independent Monte-Carlo calculations of $E_{av,ss}$ for the identical, corresponding problem. Thus, a single intersection of $\lambda(E)$ and $E_{av,ss}(\lambda)$ establishes the stability of the distribution and also yields the average energy. Note that, as with the λ = constant case of I, there is not a single 'runaway' electron. That the distribution settles down into a steady state, independent of film thickness, is seen in Fig. 2 for four different cases, labelled I through IV. For case I the independence of $E_{av,ss}$ from the initial energy E_o is also explicitly exhibited.

Note that in the E-λ plane of Fig. 1 the constant mfp situation is simply the vertical line: λ = constant. In effect, the square-root dependence of λ on E, given by (2), is just too weak a dependence to give a result qualitatively different from the λ = constant case of I.

That a single intersection of the scaling-law (1) and the $\lambda = \lambda(E)$ curve establishes a stable distribution and simultaneously gives $E_{av,ss}$ is undoubtedly true under more general circumstances than studied above. In order to explore this, we studied a model problem in which the angular scattering is also energy-dependent, namely, one corresponding to polar-optical phonon scattering as given by Eqs. (20)-(23) of I, but with the mean free path having the weak energy-dependence (2). The graphical solution exhibited in Fig. 3 for two $\lambda(E)$ cases again yields a single point of intersection for each case. Note that for polar-optical phonon

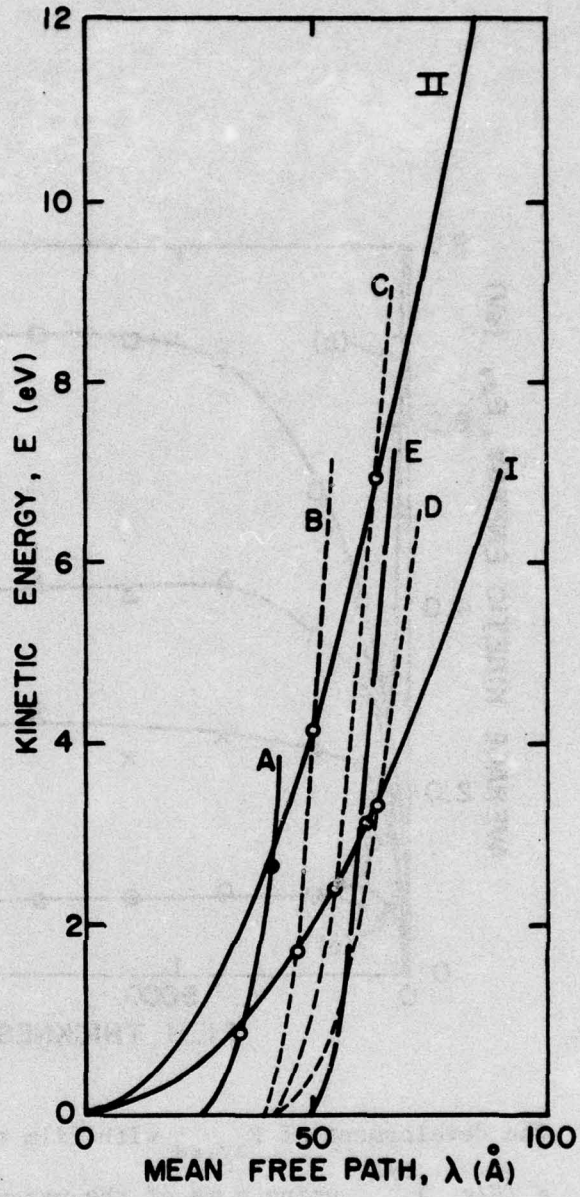

Fig. 1: Graphical determination of average steady-state energy when the mfp is a function of energy. Curves I and II are $E_{av,ss} = k\,(F\lambda)^2/\varepsilon_{ph}$ with $\varepsilon_{ph} = 0.1$ and 0.05, respectively. $F = 10^6$ V/cm and $k = 0.87$ (isotropic scattering). Curves A through E are plots of $\lambda = \lambda_o + \alpha\,(E/\varepsilon_{ph})^{1/2}$. (A) $\lambda_o = 25$ Å, $\alpha = 2$ Å; (B) $\lambda_o = 40$ Å, $\alpha = 1$ Å; (C) $\lambda_o = 40$ Å, $\alpha = 2$Å; (D) $\lambda_o = 40$ Å, $\alpha = 4$ Å; (E) $\lambda_o = 50$ Å, $\alpha = 2$Å. The open circles represent $E_{av,ss}$ computed through a Monte Carlo simulation using the parameters for scattering and for $\lambda(E)$ given by the two curves that intersect at $E_{av,ss}$.

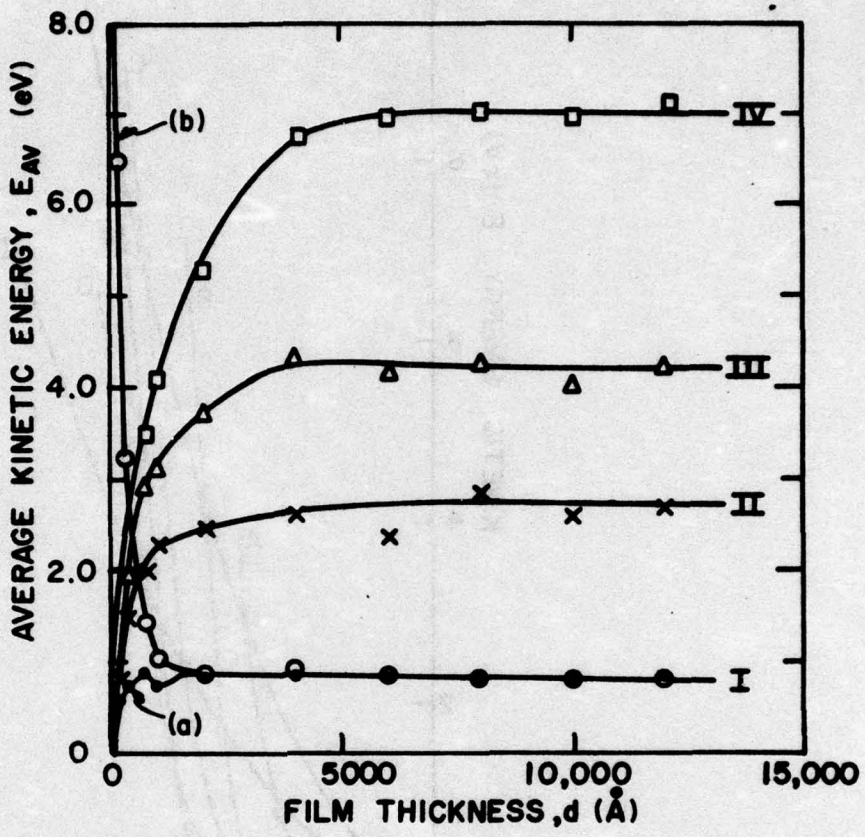

Fig. 2: The development of $E_{av,ss}$ with film thickness, d, for $\lambda = \lambda_o + \alpha (E/\varepsilon_{ph})^{1/2}$, using some of the parameters of the curves in Figure 1. $F = 10^6$ V/cm and k = 0.87 for all the curves. I (a): λ_o = 25 Å, α = 2 Å, ε_{ph} = 0.1 eV, and E_o = 0.01 eV; I (b): same as I(a), except E_o = 10 eV; II: λ_o = 25 Å, α = 2 Å, ε_{ph} = 0.05 eV, E_o = 0.01 eV; III: λ_o = 40 Å, α = 1 Å, ε_{ph} = 0.05 eV, and E_o = 0.01 eV; IV: λ_o = 40 Å, α = 2 Å, ε_{ph} = 0.05 eV, and E_o = 0.01 eV.

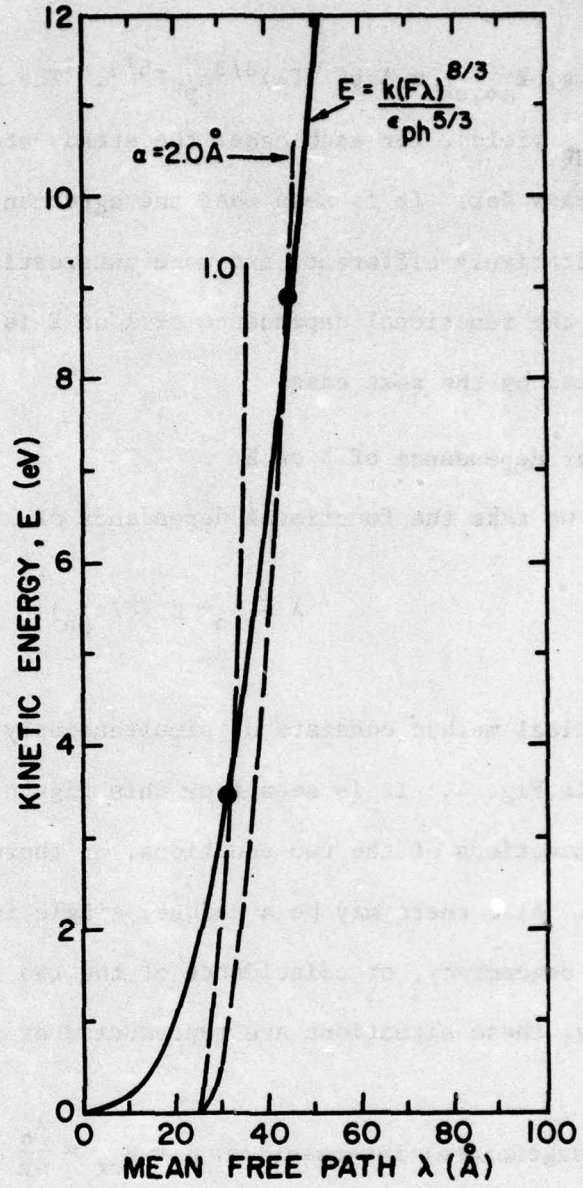

Fig. 3: Graphical determination of $E_{av,ss}$ when $E_{av,ss} = k\,(F\lambda)^{8/3}/\epsilon_{ph}^{5/3}$ and $\lambda(E) = \lambda_o + \alpha(E/\epsilon_{ph})^{1/2}$. $k = 1.64$, $F = 10^6$ V/cm, and $\epsilon_{ph} = 0.1$ eV. The form of $E_{av,ss}$ is generated using the polar-optical phonon scattering formula.

scattering, $E_{av,ss} = 1.64\ (F\lambda)^{8/3}\varepsilon_{ph}^{-5/3}$. The Monte-Carlo computation for $E_{av,ss}$ yields, for each case, the steady-state energy represented by the heavy dot. It is seen that the agreement is excellent.

Qualitatively different, and more interesting, possibilities develop if the functional dependence of λ on E is stronger. This is illustrated by the next case.

B. Linear dependence of λ on E

Here we take the functional dependence of λ on E as

$$\lambda = \lambda_o + \beta\ (E/\varepsilon_{ph}). \tag{4}$$

The graphical method consists of simultaneously plotting Eqs. (1) and (4), as in Fig. 4. It is seen from this figure that there may not be any intersections of the two equations, or there may be two intersections. Also there may be a unique, single intersection which is really a degeneracy, or coincidence of the two intersections. Algebraically, these situations are represented as follows:

Single (degenerate) intersection: $\beta = \beta_{cr} = \dfrac{\lambda_o}{4k}\left[\dfrac{\varepsilon_{ph}}{F\lambda_o}\right]^2$, (5)

$$\lambda_{cr} = 2\lambda_o\ , \qquad E_{cr} = 4k\,\frac{(F\lambda_o)^2}{\varepsilon_{ph}} = \frac{\lambda_o\,\varepsilon_{ph}}{\beta_{cr}}\ , \tag{6}$$

where (λ_{cr}, E_{cr}) are the co-ordinates of the single intersection.

No intersection: $\gamma = \dfrac{\beta}{\beta_{cr}} > 1$. (7)

Two intersections: $\gamma = \dfrac{\beta}{\beta_{cr}} < 1$. (8)

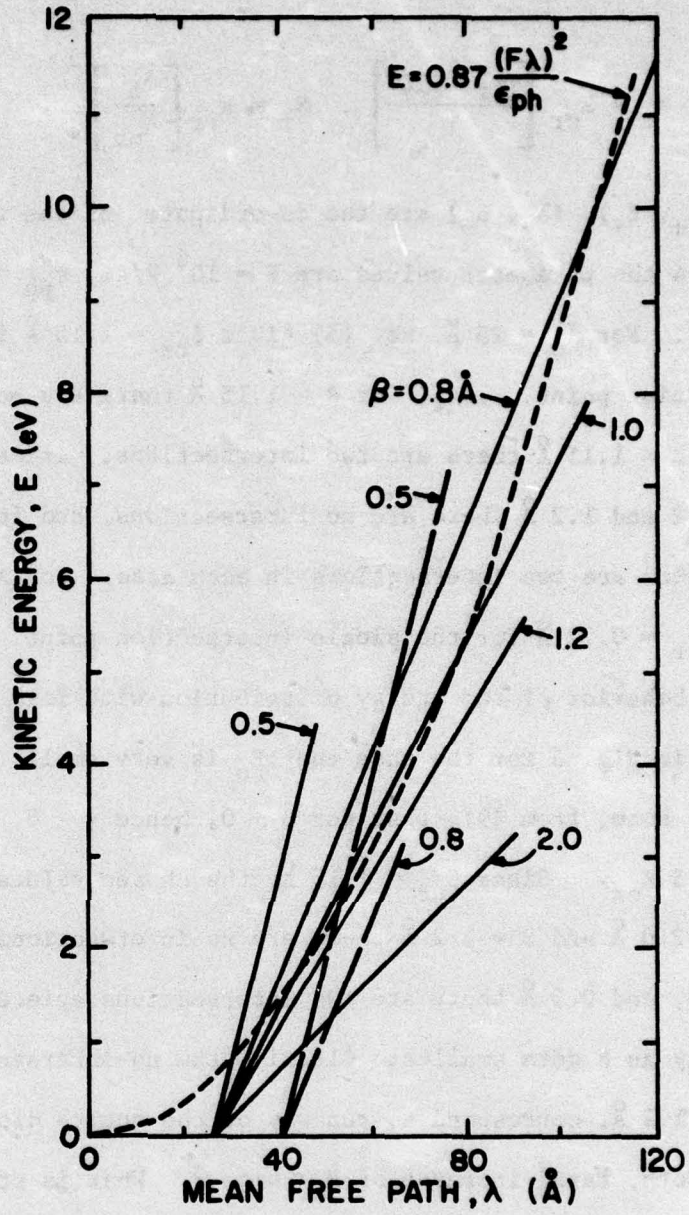

Fig. 4. Display of points of intersection between $E_{av,ss} = 0.87\ (F\lambda)^2/\varepsilon_{ph}$ and $\lambda = \lambda_o + \beta\ (E/\varepsilon_{ph})$, where $F = 10^6$ V/cm and $\varepsilon_{ph} = 0.05$ eV. Note that for some values of λ_o and β there are no intersections, which implies a runaway condition.

$$\lambda_{\pm} = \lambda_{cr}\left[\frac{1 \pm \sqrt{1-\gamma}}{\gamma}\right], \quad E_{\pm} = E_{cr}\left[\frac{\lambda_{\pm}}{\lambda_{cr}}\right]^2, \tag{9}$$

where (λ_+, E_+), (λ_-, E_-) are the co-ordinates of the two intersections. In Fig. 4 the parameter values are $F \approx 10^6$ V/cm, $\varepsilon_{ph} = 0.1$ eV and $k = 0.87$. For $\lambda_o = 25$ Å, Eq. (5) gives $\beta_{cr} = 1.15$ Å for the single intersection point. Thus, for $\beta > 1.15$ Å there are no intersections and for $\beta < 1.15$ Å there are two intersections. Indeed, it is seen that for $\beta = 2$ and 1.2 Å there are no intersections, and for $\beta = 1.0$, 0.8 and 0.5 Å there are two intersections in each case. For $\lambda_o = 40$ Å, Eq. (5) gives $\beta_{cr} = 0.72$ Å for the single intersection point.

The behavior of the energy distribution with film thickness d is studied in Fig. 5 for the case that E_o is very small ($E_o << E_- < E_{cr}$ for any β). Note, from (9), that for $\beta \to 0$, hence $\gamma \to 0$, $\lambda_- \to \lambda_{cr}/2 = \lambda_o$ and $E_- \to 0.25\, E_{cr}$. Since $\beta_{cr} = 1.15$ Å, the chosen values of β straddle β_{cr}. For $\beta = 2.0$ Å and $\beta = 1.2$ Å there are no intersections, and for $\beta = 1.0$, 0.9, 0.8, and 0.5 Å there are two intersections apiece, which separate in energy as β gets smaller. Clearly, the no-intersection cases, $\beta = 2.0$ and $\beta = 1.2$ Å, correspond to runaway of the entire distribution, exhibited by a smooth, rapid increase of E_{av} with d. What is striking about Fig. 5 is the demonstration that even with two intersections the distribution appears to be running away, namely, for $\beta = 1.0$ Å, albeit not quite as smoothly as for $\beta > \beta_{cr}$. As β gets smaller, so that E_+/E_- gets larger (see Table I) the mean energy tends more to 'settle down', though it may still increase slowly, as is seen comparing the $\beta = 1.0$, 0.9, and 0.8 Å curves in Fig. 5. Thus, the $\beta = 0.8$ Å curve is quantitatively quite different from the complete run-away curves, $\beta = 2.0$ and 1.2 Å. The

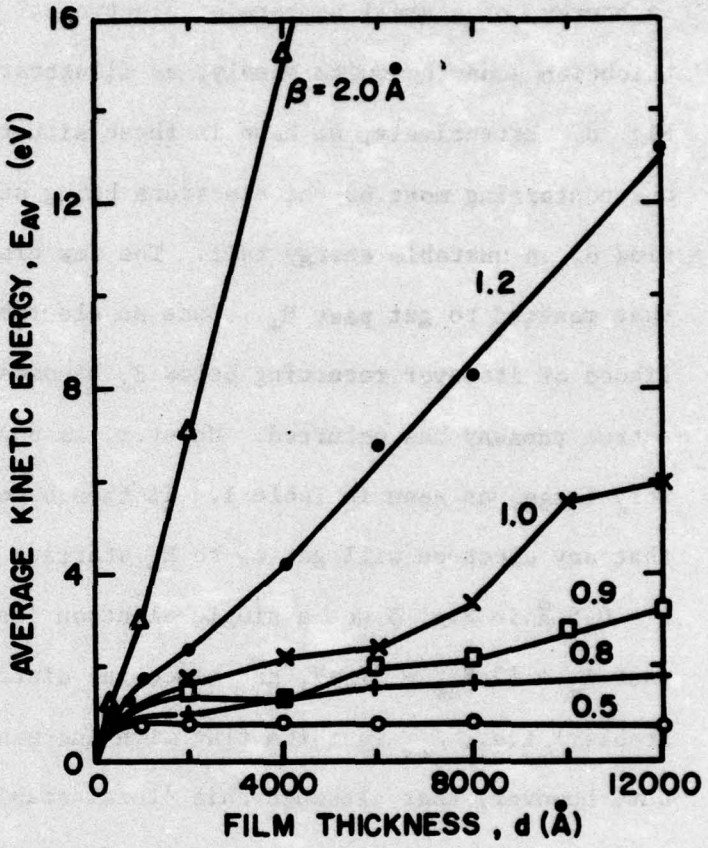

Fig. 5: The average energy of the distribution as a function of film thickness for various values of β. In all cases, λ_o = 25 Å, ε_{ph} = 0.1 eV, k = 0.87, F = 10^6 V/cm, and E_o = 0.01 eV.

β = 0.9 and 0.8 Å curves are readily interpreted in terms of the runaway, in energy, of a small numbers of electrons,[2] the remainder of the distribution behaving quite stably, as illustrated in the histogram of Fig. 6. Effectively, we have in these situations a bi-modal distribution, one containing most of the electrons being stable, and the other consisting of an unstable energy tail. The few electrons in the tail are those that managed to get past E_+. Once an electron is well past E_+, the likelihood of its ever returning below E_+ becomes vanishingly small -- that is, a true runaway has occurred. However, as β gets smaller, E_+/E_- gets very large, as seen in Table I. It then becomes increasingly unlikely that any electron will get up to E_+ starting from E_o near 0. Thus, for β = 0.5 Å in Fig. 5 not a single electron 'escaped' from the distribution, past $E_+ = 17\ E_{cr}$ = 37 eV, and hence the distribution appears to be 'totally stable,' i.e., E_{av} is quite flat with increasing d. It should be pointed out, however, that although this 'total stability' may be 'practically' true, it cannot be rigorously true. For a fixed, small β, if a large enough number of electrons are tested, i.e., if the batch number N is taken large enough, there will always be a few electrons that will run away in energy. This was simply not seen for β = 0.5 Å in Fig. 5 because N = 200 was apparently not large enough. Even a single electron running away for fixed N will prevent E_{av} from being completely flat with increasing d, as seen in the β = 0.8 and 0.9 Å curves. The case β = 1.0 Å in Fig. 5 is a transition case, in which E_+ is close enough to E_- that large numbers of electrons are running away in energy. (From Table I, $E_+ = 2.6\ E_{cr}$ = 5.7 eV and $E_- = 0.53\ E_{cr}$ = 1.2 eV). Clearly, as β increases from 1.0 Å, through β_{cr} = 1.15, to 1.2 Å, the corresponding E_{av} vs. d plots change

TABLE I

β(Å)	$\gamma = \beta/\beta_{cr}$	λ_+/λ_{cr}	E_+/E_{cr}	λ_-/λ_{cr}	E_-/E_{cr}	E_+/E_-
0.5	0.43	4.1	17.0	0.57	0.33	51
0.8	0.70	2.2	4.8	0.65	0.42	11.4
0.9	0.78	1.9	3.6	0.68	0.46	7.8
1.0	0.87	1.6	2.6	0.74	0.55	4.7
1.2	1.04	---	---	---	---	----
2.0	1.74	---	---	---	---	---

$\beta_{cr} = 1.15$ Å, $\lambda_{cr} = 50$ Å, $E_{cr} = 2.2$ eV

smoothly. In this smooth transition regime, a substnatial fraction of the total number of injected electrons runs away in energy.

From the arguments presented above it is apparent that whether or not electrons are likely to run away in energy can depend strongly on E_o, their energy at injection. This is seen strikingly in Fig. 7, in which E_{av} is plotted vs. d for $F = 10^6$ V/cm, $\varepsilon_{ph} = 0.1$ eV, $k = 0.87$ and $\lambda_o = 40$ Å. There are four curves: $E_o = 0.01$ eV and $\beta = 0.5$ and 1.0 Å, respectively; $E_o = 10$ eV and $\beta = 0.5$ and 1.0 Å, respectively. Note that $\beta_{cr} = 0.72$ Å and $E_{cr} = 5.63$ eV for the degenerate, single intersection point. Since $\beta = 1.0$ Å $> \beta_{cr}$, the two $\beta = 1$ Å curves completely run away, as expected. On the other hand, E_+/E_- is so large for $\beta = 0.5$ Å, and $E_o = 0.01$ eV that not a single electron in the batch of 200 runs away, and the average energy saturates with increasing film thickness, as with the $\beta = 0.5$ Å curve of Fig. 5. The more interesting situations are those for which $E_o = 10$ eV and $\beta < \beta_{cr}$. Thus, for $\beta = 0.5$ Å, $\gamma = \beta/\beta_{cr} = 0.693$ so that $E_+ = 28$ eV and $E_- = 2.34$ eV. Although $E_o = 10$ eV is a fair amount smaller than E_+, it is close enough that a few electrons are able to get past E_+ and run away, while all the others settle down to a much lower average energy near E_-. Note that the $\beta = 0.5$ Å curve first 'cools down' and then rises more slowly. The cooling-down phase is dominated by the main part of the distribution, which is settling down towards $E_- = 2.34$ eV from the high injection energy, $E_o = 10$ eV. The effect of the few electrons that are already running away is buried under this bulk cooling effect. However, once the bulk of the distribution has settled down, in about 5000 Å, the runaway electrons manifest themselves in a slow, steady increase in E_{av}, as seen in Fig. 7 and in Fig. 5, for the curves labelled $\beta = 0.8$ and 0.9 Å. If E_o were larger, correspondingly more electrons would run away. For $E_o >> E_+$ the entire distribution would run away. On

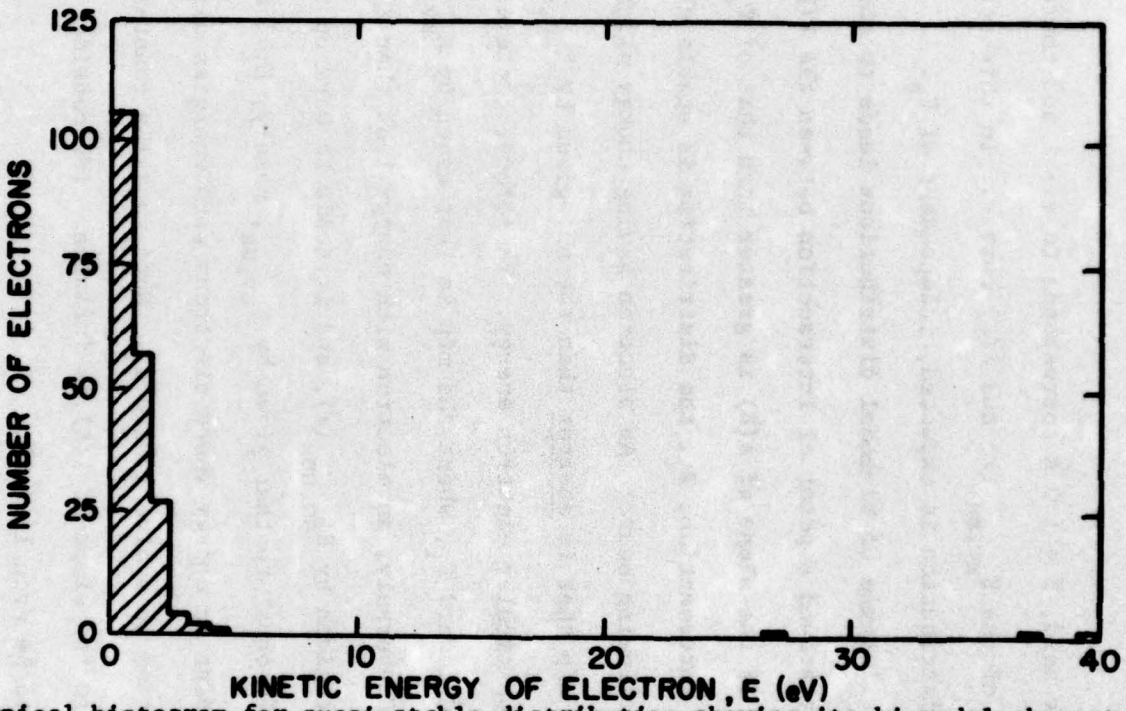

Fig. 6: Typical histogram for quasi-stable distribution, showing its bi-modal character. The parameter values are $k = 0.87$, $F = 10^6$ V/cm, $\varepsilon_{ph} = 0.1$ eV, $\lambda_o = 25$ Å, $\beta = 0.5$ Å, and $E_o = 10$ eV. The film thickness is 4000 Å. The batch size is 200 particles. Note the three runaway particles at energies above 20 eV.

the other hand, $\beta = 1.0$ Å corresponds to $\gamma > 1$ and there are no intersections of the $E_{av,ss}(\lambda)$ and $\lambda(E)$ curves. In this case runaway of the entire distribution is expected, independent of E_o.

The existence of bi-modal distributions leads to the notion of local stability around a point of intersection between the $\lambda(E)$ and $E_{av,ss}(\lambda)$ curves. If the slope of $\lambda(E)$ is greater than that of $E_{av,ss}(\lambda)$ at the point of intersection, E_i, the distribution is stable about this point in the following sense: An electron having energy slightly greater than E_i has a mfp that is <u>shorter</u> than the one given by $E_{av,ss}(\lambda)$ evaluated at that particular electron energy. Therefore, the electron tends to cool down toward E_i, where the mfp is that given by $E_{av,ss}(\lambda)$ evaluated at E_i. Conversely, an electron with energy less than E_i has a mfp <u>longer</u> than that given by $E_{av,ss}(\lambda)$, and it tends to warm up to the point where its mfp is equal to that given by $E_{av,ss}$, namely, E_i. Hence, E_i is a stable point in energy where electrons with energies differing slightly from E_i tend to evolve toward E_i. Note that λ = constant is a special case where the slope of $\lambda(E)$ is infinite. (We consider negative slopes of $\lambda(E)$ to be even larger).

When the slope of $\lambda(E)$ is less than that of $E_{av,ss}(\lambda)$ at E_i, instability results. An electron having an energy slightly above E_i has a mfp which is <u>greater</u> than that given by $E_{av,ss}(\lambda)$ evaluated at the electron energy. The electron, therefore, tends to warm up to the energy $E_{av,ss}(\lambda)$ corresponding to its mfp. As it does so, its mfp increases still further, leading to a runaway in energy. For an electron energy below E_i, the mfp is less than that given by $E_{av,ss}(\lambda)$ evaluated at the electron's energy, so that the electron tends to cool down toward an energy below E_i where $\lambda(E) = E_{av,ss}(\lambda)$. In the specific case where

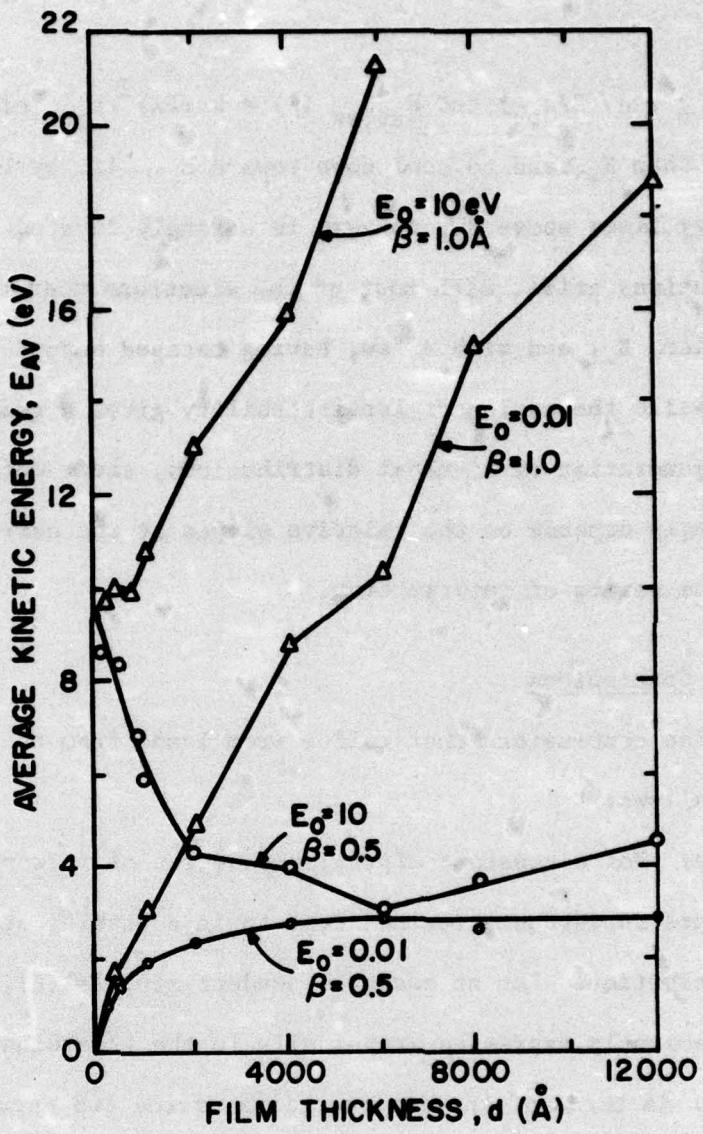

Fig. 7: The effects of initial energy, E_o, on the stability of the distribution. In all four cases, λ_o = 40 Å, k = 0.87, F = 10^6 V/cm, and ε_{ph} = 0.1 eV. A steady state is reached only for E_o = 0.01 eV and β = 0.5 Å.

$\lambda = \lambda_o + \beta\,(E/\varepsilon_{ph})$ and $E_{av,ss}(\lambda) = k\,(F\lambda)^2/\varepsilon_{ph}$, electrons with energies less than E_+ tend to cool down toward E_-. If, by chance, an electron's energy rises above E_+, runaway is strongly favored. Thus, bi-modal distributions arise, with most of the electrons near the lower point of intersection, E_-, and with a few, having escaped beyond E_+, running away.

While the notion of local stability gives a qualitative feeling for the generation of bi-modal distributions, their detailed shape, in energy, strongly depends on the relative slopes of the curves and the proximity of the points of intersection.

IV. Conclusions

The conclusions that follow from I and from the present paper are as follows:

a) For a constant mfp, λ, any degree of forward scattering, short of pure forward scattering, results in a stable, steady-state energy distribution. For an energy-dependent mfp, $\lambda=\lambda(E)$, our results are most conveniently expressed graphically in the E (ordinate), λ (abscissa) plane in terms of the intersections of the two curves $E = E_{av,ss}(\lambda)\Big|_{\lambda=\text{const}}$ and $\lambda = \lambda(E)$.

b) If there is a single intersection point (which is not a degeneracy), then a stable distribution results, with $E_{av,ss}$ given by the E_- co-ordinate of the intersection point.

c) If there are no intersection points the distribution runs away in energy.

d) If there are two intersection points the distribution is, at best, quasi-stable. That is, if the two intersection points are far enough apart

in energy, $E_+ >> E_-$, and $E_o << E_+$, the bulk of the distribution will be stable, but there may be a few runaway electrons. The closer E_o gets to E_+ the more runaway electrons there will be. In limiting cases, with both $E_- <<< E_+$ and $E_o <<< E_+$ the distribution may be stable, practically speaking; that is, the fraction of the total number of particles running away may be too miniscule to have any experimental significance.

e) More generally, an intersection point at which $\lambda=\lambda(E)$ has the steeper slope [λ = constant has infinite slope; negative slope is to be considered even steeper] promotes local stability in its vicinity. Conversely, an intersection point at which $E_{av,ss}(\lambda)$ has the steeper slope promotes local runaway in its vicinity. However, the proximity of the two intersection points is also significant in determining the entire distribution.

Finally, we should like to stress that virtually all of our studies have been based on relatively simple forms of angular scattering. We are simply not able to say whether more complicated scattering processes can lead to additional interesting results.

References

*Work supported by ARPA and monitored by AFCRL (Contract No. F19628-72-C-0298).

†Present address: Dumont Electron Tubes and Devices Corp., Clifton, N.J. 07015.

††Inactive status.

¶Present address: Department of Computer Science and Electrical Engineering, University of California, Berkeley, CA 94720

1. S. Baidyaroy, M. A. Lampert, B. Zee and R. U. Martinelli, J. Appl. Phys. 47, 2103 (1976).

2. W. Shockley, Sol. State Elec. 2, 35 (1961).